

# Rydberg Atoms in Quantum Optimization: A Review of the Maximum Independent Set Problem

Iñigo Perez Gamiz  
*Boston University*  
(Dated: May 1, 2024)

This paper aims to analyze how the Maximum Independent Set (MIS) optimization problem can be solved using Neutral Atom based quantum computers. The examination covers the implementation of some resolution methods, performance and benchmarking against classical algorithms, as well as real world applications of the problem.

## I. INTRODUCTION

Neutral Atom Quantum Computers (NAQC) are one of the most promising implementations so far in the field of Quantum Hardware, due to their unique properties and scalable potential. They use neutral atoms, typically those of alkali metals, as qubits, and manipulate these atoms using laser-induced optical tweezers and microwave pulses. Each atom is isolated and controlled in ultra-cold conditions, often near absolute zero, to minimize external interference. The quantum state of each atom is controlled by precise laser pulses, which manipulate the atomic energy states. The Rydberg state is one of these energy states and plays a crucial role in the implementation [1].

Neutral atom platforms offer several advantages over other quantum computing technologies. They inherently support large-scale qubit arrays due to the uniformity and simplicity of atomic structure, and the technology for manipulating them can be extended relatively easily. Current NAQC design is lead by companies like QuEra, that has developed a 256-qubit computer (Quera Aquila) [2], and estimates that qubit amounts of greater than 1000 will be produced soon.

As the development of Neutral Atom quantum computing hardware progresses, its applications are also becoming a central focus of study. This paper aims to analyze one of these application areas, quantum optimization, in particular the Maximum Independent Set problem.

## II. PROBLEM DEFINITION

The Maximum Independent Set (MIS) problem consists on finding the largest independent set in a graph such that all the vertices belonging to it are not connected to each other by edges. In graph theory, one particular case of graphs are the so called unit disk graphs, in which every vertex is only connected to all the vertices contained within unit distance, as shown in Figure (1). For this type of

graphs, finding the exact solution to the MIS problem is considered to be an NP-hard problem in the worst scenario. So far, there are only approximation algorithms that run in polynomial time [3].

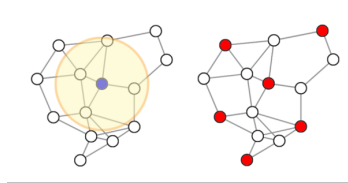


FIG. 1. MIS for unit disk graphs [4].

## III. USE OF RYDBERG ATOM ARRAYS

Unit disk graphs and their MIS problem solution can be implemented using Rydberg atom arrays. For a given graph, a geometric configuration of atoms is created, where every atom corresponds to a vertex, and the unit distance is considered to be the Rydberg blockade radius  $R_b$ . If an atom is in the Rydberg state  $|1\rangle$ , that means that the vertex belongs to the Maximum Independent Set, and if it is in the ground state  $|0\rangle$ , it does not belong. According to the Rydberg blockade mechanism, it is prohibited to have more than one atom in the Rydberg state within  $R_b$  distance due to strong interactions. Therefore, the blockade mechanism naturally imposes a constraint that satisfies the independent set condition: if a vertex is in the set (Rydberg state), any vertex connected to it by an edge cannot be also in the set. Thus the MIS problem can be translated into finding the maximum set of atoms that can simultaneously be in the Rydberg state without violating the blockade constraint.

For this paper, it will be assumed that 80% of the arrays are filled, and that each atom is connected to its nearest neighbors and next nearest neighbors (diagonal) [4].

#### IV. VARIATIONAL QUANTUM OPTIMIZATION ALGORITHMS

Quantum optimization algorithms are usually implemented through global atomic excitation using homogeneous laser pulses that have a time-dependent Rabi frequency and phase  $\Omega(t)e^{i\phi(t)}$ , and a detuning  $\Delta(t)$ . A general Hamiltonian that describes the MIS problem  $H = H_D + H_C$  is composed of a driver Hamiltonian  $H_D$  that represents the dynamics of the system, and a cost Hamiltonian  $H_C$ .

$$H_D = \frac{\hbar}{2} \sum_i \Omega(t) \left( e^{i\phi(t)} |0\rangle_i \langle 1| + e^{-i\phi(t)} |1\rangle_i \langle 0| \right) \quad (1)$$

$$H_C = -\hbar\Delta(t) \sum_i n_i + \sum_{i < j} V_{ij} n_i n_j \quad (2)$$

Here  $n_i = \sum_i |1\rangle_i \langle 1|$  represents an atom in the Rydberg state, and  $V_{ij} = V_0/|r_i - r_j|^6$  is the interaction potential given by the blockade mechanism. As every optimization problem, the objective is to minimize the cost function (in this case Hamiltonian), that is, maximize the number of atoms in the Rydberg state  $\sum_i n_i$  while keeping the interaction potential low [4].

Two variational quantum optimization algorithms are used together with a classical optimization forming a loop. The schema can be visualized in Figure 2. Both algorithms follow the same procedure. Initially, the atoms are placed in the location of the vertices, all in the ground state. The system then evolves according to a specific choice of variational parameters  $U(\Omega(t), \phi(t), \Delta(t))$ , to later sample the system wavefunction with a projective measurement, determining the number of atoms in the Rydberg state  $\sum_i n_i$ . This process is repeated many times to estimate the average size of the Maximum Independent Set  $\langle \sum_i n_i \rangle$ , the approximation ratio  $R = \langle \sum_i n_i \rangle / |\text{MIS}|$  and the probability of finding the solution to the problem. There is also a classical optimizer that tries to update the variational parameters every loop in order to maximize  $\sum_i n_i$ .

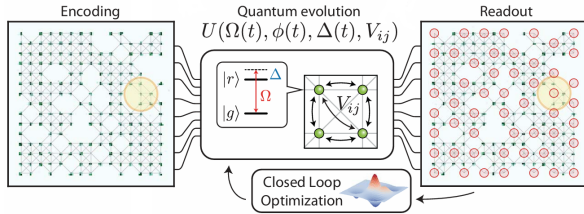


FIG. 2. Quantum-classical optimization loop [4].

#### A. QAOA

The first implemented algorithm is the Quantum Approximate Optimization Algorithm (QAOA). This is a parametrized algorithm that evolves in  $p$  layers under the influence of non-commuting Hamiltonians  $H_B$  and  $H_C$  (cost Hamiltonian) [5]

$$|\psi\rangle = e^{-iH_B\beta_p} e^{-iH_C\gamma_p} \dots e^{-iH_B\beta_1} e^{-iH_C\gamma_1} |\psi_0\rangle \quad (3)$$

The system starts in  $|\psi\rangle = |\psi_0\rangle$ , an eigenvector of  $H_B$ , and the objective is to find the ground state of the Hamiltonian (minimize cost function) using the  $2p$  variational parameters  $(\gamma_1, \dots, \gamma_p), (\beta_1, \dots, \beta_p)$ .

For the particular case of the MIS,  $H_C$  is the same as (2), but without the Rydberg interaction term, that is introduced into  $H_B$ .

$$H_B = \frac{\hbar}{2} \sum_i \Omega (|0\rangle_i \langle 1| + |1\rangle_i \langle 0|) + \sum_{i < j} V_{ij} n_i n_j \quad (4)$$

$$H_C = -\hbar\Delta(t) \sum_i n_i \quad (5)$$

The initial state is  $|\psi_0\rangle = |00\dots 0\rangle$ , the ground state of  $H_C$  for an initial  $\Delta < 0$ . Evolution under  $H_B$  is implemented using a laser whose pulses vary along  $p$  time layers  $(\tau_1, \dots, \tau_p)$ , keeping the Rabi frequency constant and  $\Delta = 0$ . At the same time, evolution under  $H_C$  is implemented introducing a phase jump in each laser pulse layer  $(\phi_1, \dots, \phi_p)$ , and it represents a global Z-rotation of atoms in the Rydberg state. As a result, the algorithm has a total of  $2p-1$  parameters  $(\tau_1, \dots, \tau_p), (\phi_2, \dots, \phi_p)$ , since  $e^{-iH_C\phi_1}$  has no effect on the initial state [5].

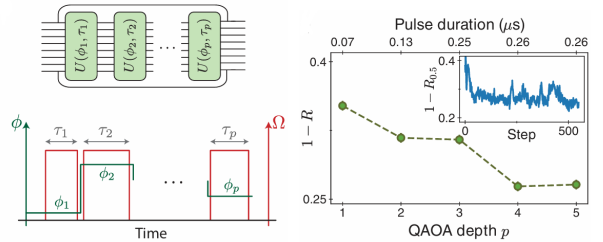


FIG. 3. QAOA schema and performance against  $p$  [4].

The performance of the QAOA as a function of the number of layers can be visualized in Figure 3. The approximation ratio  $R$  increases until  $p = 4$ , and from there the performance does not improve as  $p$  grows. This could be due to several factors, including the difficulty to optimize a greater number of parameters, next nearest neighbors Rydberg blockade violations and laser imperfections.

## B. VQAA

The second approach is the Variational Quantum Adiabatic Algorithm (VQAA), that aims to find the best quasi-adiabatic path from an initial Hamiltonian with a trivial ground state to a final Hamiltonian whose ground state is the solution to the problem. For the case of the MIS problem, the VQAA tries to optimize a time-varying detuning  $\Delta(t)$  from negative to positive values keeping a constant Rabi frequency  $\Omega$ . The detuning is parametrized as a piecewise linear function, with an initial value  $\Delta_0$  and  $f$  linear segments defined by their time duration  $(\tau_1, \dots, \tau_f)$  and end value  $(\Delta_1, \dots, \Delta_f)$ . The Rabi frequency is initialized in a time interval  $\tau_\Omega$  at a constant  $\Delta_0$ , and is also deactivated in a time interval  $\tau_\Delta$  at a constant  $\Delta_f$  (Figure 4). This gives a total of  $2f+3$  variational parameters  $(\tau_1, \dots, \tau_f), (\Delta_1, \dots, \Delta_f), (\Delta_0, \tau_\Delta, \tau_\Omega)$ . For the VQAA, the effective circuit depth  $\tilde{p}$  is defined as the quotient between the duration of a sweep  $T = \tau_1 + \dots + \tau_f$  and  $\tau_\pi$ , that is the duration of the pulse required to excite an atom [5].

The results of the VQAA can be visualized in Figure 4. With only  $f = 3$  segments, an optimal sweep of duration  $T = 1.25\mu s$  that corresponds to an effective depth of  $\tilde{p} = 10$ , gives better results than the best result of the QAOA (higher  $R$ ). At the same time, as the value of  $\tilde{p}$  increases from a value of 15, the performance decreases, probably due to decoherence in the laser.

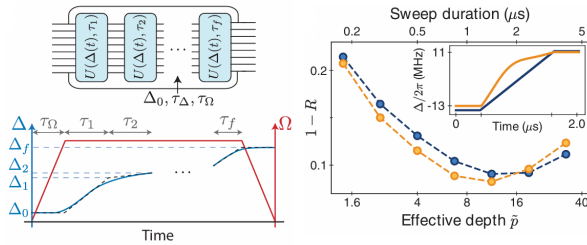


FIG. 4. VQAA schema and performance against  $\tilde{p}$  [4].

The optimized VQAA is applied to 115 different graphs of sizes  $N$  ranging from 80 to 289 vertices. For graphs of the same size (180 in Figure 5), the approximation error  $1 - R$  decreases and the probability of finding a solution  $P_{MIS}$  increases with  $\tilde{p}$  up to  $\tilde{p} \approx 10$  (Figure 5A). At the same time, there is a strong correlation between the performance of the algorithm and the MIS degeneracy  $D_{|MIS|}$ , as shown in Figure 5B. The relation between  $1 - R$  and  $\rho \equiv \log(D_{|MIS|})/N$  is linear (Figure 5C), being  $\rho$  the degeneracy density that measures the difficulty to find solutions at shallow depths [4].

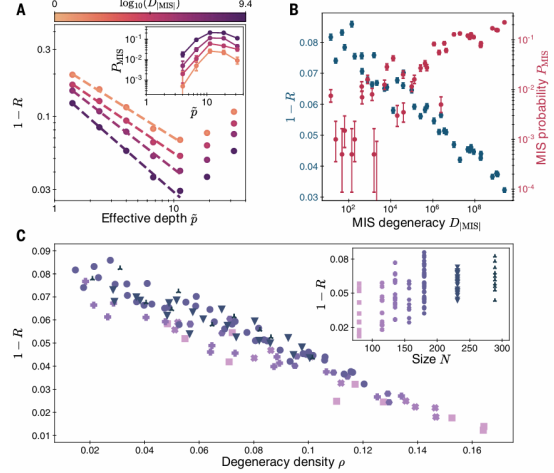


FIG. 5. VQAA performance on different graphs [4].

## V. BENCHMARKING AGAINST SA

After analyzing the performance of the VQAA, it is interesting to benchmark the results against a classical algorithm, in this case Simulated Annealing (SA). This classical algorithm aims to find the ground state of a cost Hamiltonian by imitating the cooling of an interacting system of spins. The algorithm stochastically changes the system spin state in  $\{|0\rangle, |1\rangle\}^N$  based on a probability of transition matrix that depends on a temperature  $\beta^{-1}$  and the system Hamiltonian. After many spin updates, the algorithm stabilizes to a stationary configuration that is the problem solution.

For the case of the MIS problem, the spin states represent if a vertex is in the set or not ( $|1\rangle$  yes,  $|0\rangle$  not). The Hamiltonian that encodes the problem is

$$H_C^{SA} = - \sum_i n_i + \sum_{i < j} \alpha n_i n_j, \quad \alpha > 0 \quad (6)$$

The algorithm operates as follows. Initially, all the spins are in state  $|0\rangle$ , that is, no vertex is in the set. Each time, a vertex is randomly chosen. If it does not belong to the set, then it is added to it with probability 1. If otherwise it was already in the set, there are 3 possibilities: (a) Remove the vertex from the set with probability  $\epsilon$ . (b) Exchange state/spin with a neighbor with probability  $(1-\epsilon)/8$  for each neighbor. (c) No change with the remaining probability. Here  $\epsilon$  is a parameter that needs to be optimized. The variation in energy  $\Delta E$  under the cost Hamiltonian for the proposed change is computed and the update is accepted with probability  $e^{-\beta \Delta E}$  if  $\Delta E \geq 0$ , and 1 if  $\Delta E < 0$ . The mean number of attempted updates per spin is the depth of the algorithm  $p_{SA}$  [5].

The VQAA and SA results are compared in Figure 6. For relatively shallow depths and not very hard graphs (green and gray), the approximation errors are similar. For harder graphs (purple and gold) with low degeneracy  $\rho$ , Simulated Annealing shows a plateau in the approximation error at  $R = |\text{MIS}| - 1/|\text{MIS}|$ , indicating that the algorithm gets stuck in local minima that correspond to configurations that have one less vertex than the optimal solution. VQAA quickly finds the optimal solution in the gold curve, but also struggles in approaching the purple correct solution as the  $P_{\text{MIS}}$  plot shows. It is also true that SA, even if it requires greater circuit depths, is capable of reaching smaller approximation rates than VQAA. However, the approximation error for the VQAA is not big enough to prevent it from finding the correct solution (e.g. if the actual solution size is 18, providing 17 as solution is a bigger error than 0.05).

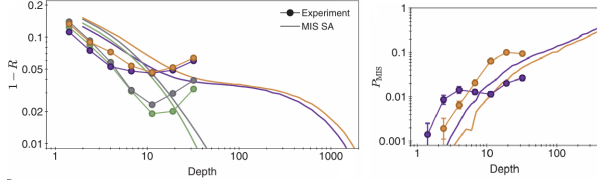


FIG. 6. VQAA and SA performance for four 80-vertex graphs. Green ( $\mathcal{HP} = 1.8, \rho = 0.13$ ) and Gray ( $\mathcal{HP} = 2.1, \rho = 0.11$ ) are easy. Purple ( $\mathcal{HP} = 69, \rho = 0.08$ ) and Gold ( $\mathcal{HP} = 68, \rho = 0.06$ ) are hard [4].

A useful parameter that determines the difficulty of finding the actual optimal solution is the "hardness parameter"  $\mathcal{HP} = D_{|\text{MIS}|-1}/|\text{MIS}|$ , that was found to exponentially increase with  $\sqrt{N}$  for the most difficult graphs. After an in-depth study, it was discovered that for Simulated Annealing, the probability of finding the MIS solution scales as  $P_{\text{MIS}} = \exp(-C\mathcal{HP}^{-1.03(4)})$ . On the other hand, the quantum algorithm seemed to generally scale very similar,  $P_{\text{MIS}} = \exp(-C\mathcal{HP}^{-0.95(15)})$ , but there were graphs in which it could improve its performance to  $P_{\text{MIS}} = \exp(-C\mathcal{HP}^{-0.63(13)})$ , clearly beating the classical one. This best scenario is reached when graphs satisfy the deep-circuit-regime  $T > 1/\delta_{\min}$ , where  $\delta_{\min}$  is the minimum energy gap during the adiabatic evolution [4].

## VI. APPLICATIONS OF THE MIS

To understand the interest in exploring the use of quantum computers to solve the Maximum Independent Set problem, it is important to know the real-world applications it has. The MIS problem can be

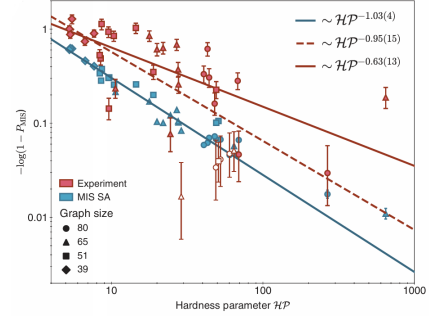


FIG. 7.  $P_{\text{MIS}}$  scaling with  $\mathcal{HP}$  [4].

applied for optimization accross different industries, including [6]:

- Antenna placement optimization, with the objective of maximizing coverage while minimizing interference between antennas.
- Portfolio optimization, to maximize returns while managing risk by selecting a set of stocks (or assets) that are not closely correlated.
- Network optimization, to minimize the number of nodes that need to be controlled while still maintaining the network's functionality.

Given the relevance of the applications, research on the topic will continue and get intensified in upcoming years.

## VII. CONCLUSION

The nature of Neutral Atom computers creates a suitable environment to solve the Maximum Independent Set problem. In this context, variational quantum optimization algorithms that aim to solve the problem are analyzed. The Variational Quantum Adiabatic Algorithm shows a better performance than the Quantum Approximate Optimization Algorithm. After applying the optimized VQAA to several graphs, it is observed that its approximation rate increases with the effective circuit depth up to  $\tilde{p} = 10$ , and that it is strongly correlated with the problem degeneracy. This optimized algorithm is also benchmarked against a classical Simulated Annealing, finding that the quantum algorithm could quickly find the correct solution for some graphs in which Simulated Annealing got stuck in local minima. It was also found that the VQAA provides a better scaling in the probability of finding a solution if the deep-circuit-regime is satisfied.

- 
- [1] Karen Wintersperger, Florian Dommert, Thomas Ehmer, Andrey Hoursanov, Johannes Klepsch, Wolfgang Mauere, Georg Reuber, Thomas Strohm, Ming Yin, and Sebastian Lubert. Neutral atom quantum computing hardware: performance and end-user perspective. *EPJ Quantum Technology*, 10(1), August 2023.
  - [2] Jonathan Wurtz, Alexei Bylinskii, Boris Braverman, Jesse Amato-Grill, Sergio H. Cantu, Florian Huber, Alexander Lukin, Fangli Liu, Phillip Weinberg, John Long, Sheng-Tao Wang, Nathan Gemelke, and Alexander Keesling. Aquila: Quera’s 256-qubit neutral-atom quantum computer, 2023.
  - [3] Ruben S. Andrist, Martin J. A. Schuetz, Pierre Minssen, Romina Yalovetzky, Shouvanik Chakrabarti, Dylan Herman, Niraj Kumar, Grant Salton, Ruslan Shaydulin, Yue Sun, Marco Pistoia, and Helmut G. Katzgraber. Hardness of the maximum-independent-set problem on unit-disk graphs and prospects for quantum speedups. *Physical Review Research*, 5(4), December 2023.
  - [4] S. Ebadi, A. Keesling, M. Cain, T. T. Wang, H. Levine, D. Bluvstein, G. Semeghini, A. Omran, J.-G. Liu, R. Samajdar, X.-Z. Luo, B. Nash, X. Gao, B. Barak, E. Farhi, S. Sachdev, N. Gemelke, L. Zhou, S. Choi, H. Pichler, S.-T. Wang, M. Greiner, V. Vuletić, and M. D. Lukin. Quantum optimization of maximum independent set using rydberg atom arrays. *Science*, 376(6598):1209–1215, June 2022.
  - [5] S. Ebadi, A. Keesling, M. Cain, T. T. Wang, H. Levine, D. Bluvstein, G. Semeghini, A. Omran, J.-G. Liu, R. Samajdar, X.-Z. Luo, B. Nash, X. Gao, B. Barak, E. Farhi, S. Sachdev, N. Gemelke, L. Zhou, S. Choi, H. Pichler, S.-T. Wang, M. Greiner, V. Vuletić, and M. D. Lukin. Supplementary materials for quantum optimization of maximum independent set using rydberg atom arrays. *Science*, 376(6598):1209–1215, June 2022.
  - [6] Jonathan Wurtz, Pedro L. S. Lopes, Christoph Gorgulla, Nathan Gemelke, Alexander Keesling, and Shengtao Wang. Industry applications of neutral-atom quantum computing solving independent set problems, 2024.